



## OPEN ACCESS

## EDITED BY

Kang Cui,  
University of Jinan, China

## REVIEWED BY

Forough Ghasemi,  
Agricultural Biotechnology Research Institute of  
Iran, Iran  
Javeed Mahmood,  
King Abdullah University of Science and  
Technology, Saudi Arabia

## \*CORRESPONDENCE

Umar Nishan,  
✉ umarnishan85@gmail.com  
Ke Chen,  
✉ chen\_ke@swwmu.edu.cn

RECEIVED 15 November 2023

ACCEPTED 29 January 2024

PUBLISHED 08 February 2024

## CITATION

Nishan U, Zahra T, Badshah A, Muhammad N,  
Afridi S, Shah M, Khan N, Asad M, Ullah R, Ali EA  
and Chen K (2024), Colorimetric sensing of  
hydrogen peroxide using capped *Morus nigra*-  
sawdust deposited zinc oxide nanoparticles via  
*Trigonella foenum* extract.  
*Front. Bioeng. Biotechnol.* 12:1338920.  
doi: 10.3389/fbioe.2024.1338920

## COPYRIGHT

© 2024 Nishan, Zahra, Badshah, Muhammad,  
Afridi, Shah, Khan, Asad, Ullah, Ali and Chen. This  
is an open-access article distributed under the  
terms of the [Creative Commons Attribution  
License \(CC BY\)](https://creativecommons.org/licenses/by/4.0/). The use, distribution or  
reproduction in other forums is permitted,  
provided the original author(s) and the  
copyright owner(s) are credited and that the  
original publication in this journal is cited, in  
accordance with accepted academic practice.  
No use, distribution or reproduction is  
permitted which does not comply with  
these terms.

# Colorimetric sensing of hydrogen peroxide using capped *Morus nigra*-sawdust deposited zinc oxide nanoparticles via *Trigonella foenum* extract

Umar Nishan<sup>1\*</sup>, Tabassum Zahra<sup>1</sup>, Amir Badshah<sup>1</sup>,  
Nawshad Muhammad<sup>2</sup>, Saifullah Afridi<sup>1</sup>, Mohibullah Shah<sup>3</sup>,  
Naeem Khan<sup>1</sup>, Muhammad Asad<sup>1</sup>, Riaz Ullah<sup>4</sup>, Essam A. Ali<sup>5</sup> and  
Ke Chen<sup>6\*</sup>

<sup>1</sup>Department of Chemistry, Kohat University of Science and Technology, Kohat, Pakistan, <sup>2</sup>Department of Dental Materials, Institute of Basic Medical Sciences Khyber Medical University, Peshawar, Pakistan, <sup>3</sup>Department of Biochemistry, Bahauddin Zakariya University, Multan, Pakistan, <sup>4</sup>Department of Pharmacognosy, College of Pharmacy, King Saud University, Riyadh, Saudi Arabia, <sup>5</sup>Department of Pharmaceutical Chemistry, College of Pharmacy, King Saud University Riyadh, Riyadh, Saudi Arabia, <sup>6</sup>Department of Infectious Diseases, The Affiliated Hospital of Southwest Medical University, Luzhou, China

Hydrogen peroxide (H<sub>2</sub>O<sub>2</sub>) is one of the main byproducts of most enzymatic reactions, and its detection is very important in disease conditions. Due to its essential role in healthcare, the food industry, and environmental research, accurate H<sub>2</sub>O<sub>2</sub> determination is a prerequisite. In the present work, *Morus nigra* sawdust deposited zinc oxide (ZnO) nanoparticles (NPs) were synthesized by the use of *Trigonella foenum* extract via a hydrothermal process. The synthesized platform was characterized by various techniques, including UV-Vis, FTIR, XRD, SEM, EDX, etc. FTIR confirmed the presence of a Zn–O characteristic peak, and XRD showed the hexagonal phase of ZnO NPs with a 35 nm particle size. The EDX analysis confirmed the presence of Zn and O. SEM images showed that the as-prepared nanoparticles are distributed uniformly on the surface of sawdust. The proposed platform (acetic acid-capped ZnO NPs deposited sawdust) functions as a mimic enzyme for the detection of H<sub>2</sub>O<sub>2</sub> in the presence of 3,3',5,5'-tetramethylbenzidine (TMB) colorimetrically. To get the best results, many key parameters, such as the amount of sawdust-deposited nanoparticles, TMB concentration, pH, and incubation time were optimized. With a linear range of 0.001–0.360 μM and an R<sup>2</sup> value of 0.999, the proposed biosensor's 0.81 nM limit of quantification (LOQ) and 0.24 nM limit of detection (LOD) were predicted, respectively. The best response for the proposed biosensor was observed at pH 7, room temperature, and 5 min of incubation time. The acetic acid-capped sawdust deposited ZnO NPs biosensor was also used to detect H<sub>2</sub>O<sub>2</sub> in blood serum samples of diabetic patients and suggest a suitable candidate for *in vitro* diagnostics and commercial purposes.

## KEYWORDS

diabetes, cancer, TMB, hydrothermal process, colorimetric biosensing

## 1 Introduction

Hydrogen peroxide ( $H_2O_2$ ) monitoring in diverse matrices has crucial roles in cell metabolism and has diverse applications in industrial processes (Zhang et al., 2018).  $H_2O_2$  is used in medical diagnostics, clinical research and industrial sectors including textiles, paper, pharmaceuticals, food processing, cleaning, disinfection, etc (Patel et al., 2020). Additionally, in the biosystem, it regulates metabolic activity, cell apoptosis, immune cell activation, and different physiological processes (Miller et al., 2010). It serves as an oxidative agent, a stress marker, and a cell defensive agent. Similarly, it is an important biomarker for a variety of diseases and disorders, including cardiovascular, Alzheimer's, Parkinson's, diabetes, and neurodegenerative disorders (Rao and Balachandran, 2002). Furthermore,  $H_2O_2$  is a byproduct of lactate, alcohol, glucose, glutamate, and cholesterol oxidases. In the past,

different detection methods for  $H_2O_2$  quantifications were applied. These include chemiluminescence (Irani-nezhad et al., 2019), chromatography (Nakashima et al., 1994), electrochemistry (Lee et al., 2016), fluorescence (Senthamizhan et al., 2016), electrochemical methods, etc (Chen et al., 2014). However, most of these approaches are toxic to living cells, thus making them ineffective for *in situ*  $H_2O_2$  detection in biological materials. Besides, some of these techniques are time-consuming, expensive, and complex, restricting their application in laboratories with limited resources (Nishan et al., 2021a). Conversely, in comparison to other complex approaches, colorimetric methods for detecting  $H_2O_2$  have been getting key attention nowadays due to their easy handling and low cost. The progress of colorimetric reactions can be monitored with the naked eye (Khalik et al., 2023).

Cellulose is the main constituent of sawdust. It is one of the most abundant, natural, renewable, biocompatible, and environmentally

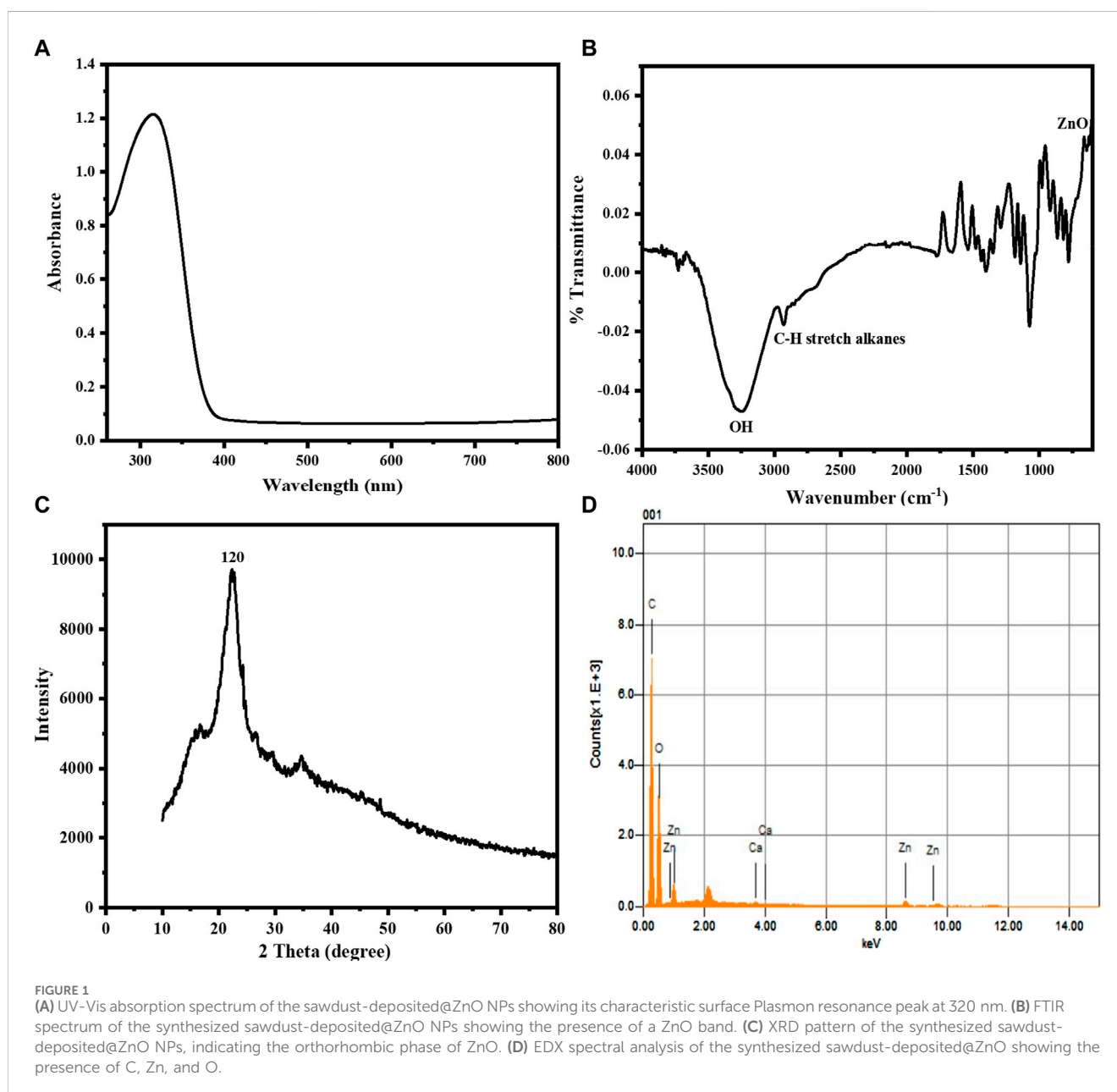


TABLE 1 EDX elemental analysis of the synthesized sawdust-deposited@ZnO

Element	Weight %	Atomic %
C	49.90	58.45
O	46.95	40.71
Ca	0.17	0.06
Zn	3.64	0.78
Total	100.00	100.00

friendly macromolecules (Park et al., 2019). Cellulosic materials have adaptable surface characteristics, low cost, better mechanical properties, a higher aspect ratio, a lower density, a higher surface area, and a lower density. Cellulose-based sawdust has been utilized as a sacrificial porous template because it is non-edible, cheap, renewable, and readily available biomass (Khaliq et al., 2023).

Various nanomaterials, including positively charged gold nanoparticles (Jv et al., 2010), CuS nanoparticles (Dutta et al., 2013), graphene oxide (Song et al., 2010), ceria nanoparticles (Ornatska et al., 2011), cupric oxide nanoparticles (Chen et al., 2011), and CoFe<sub>2</sub>O<sub>4</sub> NPs (Shi et al., 2011), have been found to

exhibit peroxidase-like activity and are employed to detect H<sub>2</sub>O<sub>2</sub> visually. Additionally, acetic acid-capped ZnO NPs are recyclable, highly stable, and efficient, have good sensing and catalytic capabilities, and have a tremendous potential to replace expensive noble metal NPs in biosensing. Because ZnO NPs have a large band gap (3.3 eV), they can be employed for UV luminescence at room temperature (Khranovskyy et al., 2012). Furthermore, ZnO NPs have a high isoelectric point (pI) of 9.5, allowing effective immobilization of enzymes with a low pI, i.e., ≤5 (Wei et al., 2010). ZnO NPs are also biocompatible, have the largest family of nanostructures, are crystalline, and have a high surface-to-volume ratio (Abou Chaaya et al., 2014).

In the present study, the hydrothermal method was used for the synthesis of *Morus nigra*-deposited ZnO NPs with the use of *Trigonella foenum* extract as a reductant. To further improve their sensing abilities, the synthesized NPs were capped with acetic acid. The oxidation of chromogenic substrate, i.e., TMB, by H<sub>2</sub>O<sub>2</sub> in the presence of acetic acid-capped sawdust deposited@ZnO is being reported for the first time. The proposed platform is a new, simple, quick, highly sensitive, and selective approach for H<sub>2</sub>O<sub>2</sub> detection. The amount of capped NPs, pH, TMB concentration, and incubation time were among the various reaction parameters that were adjusted to achieve the best performance out of the suggested

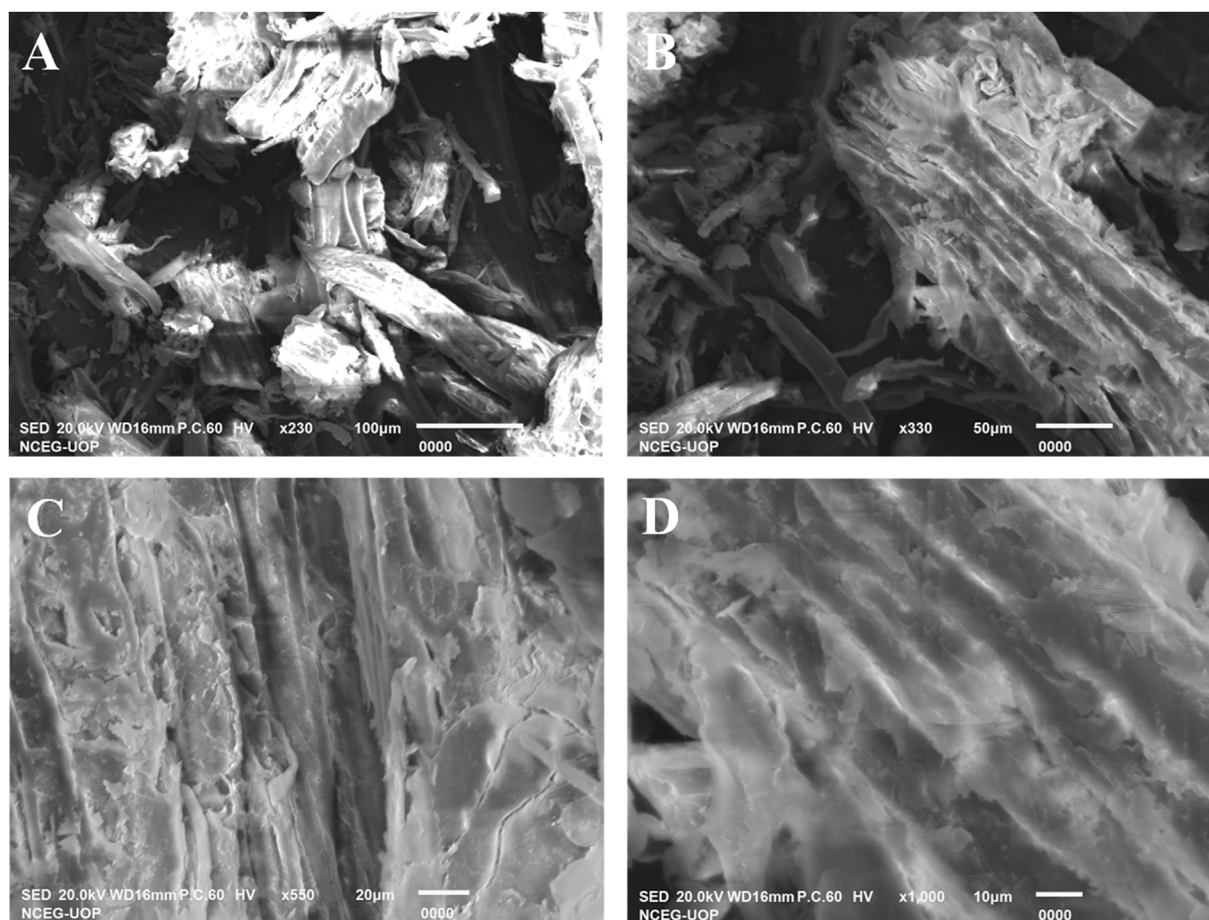
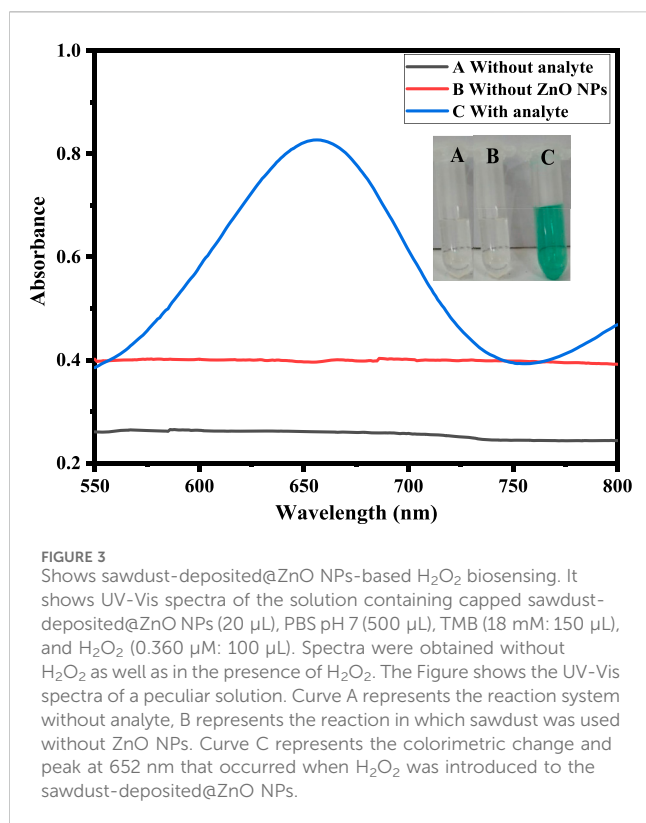


FIGURE 2 SEM images (A–D) were taken at different magnifications. The results depict that the nanoparticles are distributed uniformly over the surface of sawdust to enhance its catalytic activity.



sensor. The sensitivity and selectivity were also investigated under the aforementioned optimum conditions. Finally, H<sub>2</sub>O<sub>2</sub> levels were also measured in blood serum samples to testify to the fabricated platform.

## 2 Experimental procedure

### 2.1 Materials and reagents

In the entire experimental procedure, all chemicals used were of analytical grade, and no further purification was performed. Double-distilled water was used in the preparation of solutions. NaOH (97%), HCl (37%), acetic acid (97%), ascorbic acid (97%), urea (99.5%), and 3,3',5,5'-tetramethylbenzidine (TMB) were procured from Daejung, South Korea. KGaA and H<sub>2</sub>O<sub>2</sub> (35%) were purchased from Merck. The collection of blood serum was performed at a local lab close to the divisional teaching hospital in Kohat, KP, from three diabetic individuals. The serum was twice diluted with a PBS solution to decrease the complexity of the matrix, according to the earlier reports (Singh et al., 2022).

### 2.2 Instrumentation

Fourier transform infrared spectroscopy (FTIR, Nicolet 6,700, US) was used to find the characteristic peaks of the synthesized platform in the range of 4,000–500 cm<sup>-1</sup>. The morphology of the synthesized NPs was confirmed using a scanning electron microscope (SEM) with INCAx-act Oxford Instruments

(TESCAN VEGA (LMU)). X-ray diffraction was used to identify the phases of the produced ZnO NPs (JCPDS, file No. 04-0783). The absorption spectra were taken with a Shimadzu UV-Vis spectrophotometer (1,800, Japan).

### 2.3 Synthesis of Sawdust-deposited@ZnO NPs

The green leaves of *T. foenum* were collected, washed with distilled water, and dried in sunlight for 4 days. The leaves were ground into a fine powder with the help of a blender. Extract was prepared in distilled water by suspending 5 g of leaf powder in 200 mL of distilled water on a hot plate with a magnetic stirrer (1,000 rpm) for 1 h at 65°C. The mixture was filtered, and the extract was poured into a beaker. One Gram of zinc acetate was dissolved in 50 mL of distilled water and placed on a hot plate. Subsequently, 50 mL of extract solution was added dropwise to the zinc acetate solution, and 1 g of sawdust from *M. nigra* was gradually added while stirring at 65°C for 4 h. The synthesized sawdust-deposited@ZnO NPs solution was centrifuged for 15 min at 4,500 rpm to obtain solid material.

### 2.4 Capping of sawdust-deposited@ZnO NPs with acetic acid

The Sawdust-deposited@ZnO NPs were capped with an acetic acid solution such that 0.12 g of the mimic enzyme was mixed with 2 mL of acetic acid for 30 min through a mortar and pestle thoroughly. It resulted in the formation of a brown mixture that was placed in an Eppendorf tube for further use (Asad et al., 2022; Nishan et al., 2022).

### 2.5 Colorimetric sensing of H<sub>2</sub>O<sub>2</sub>

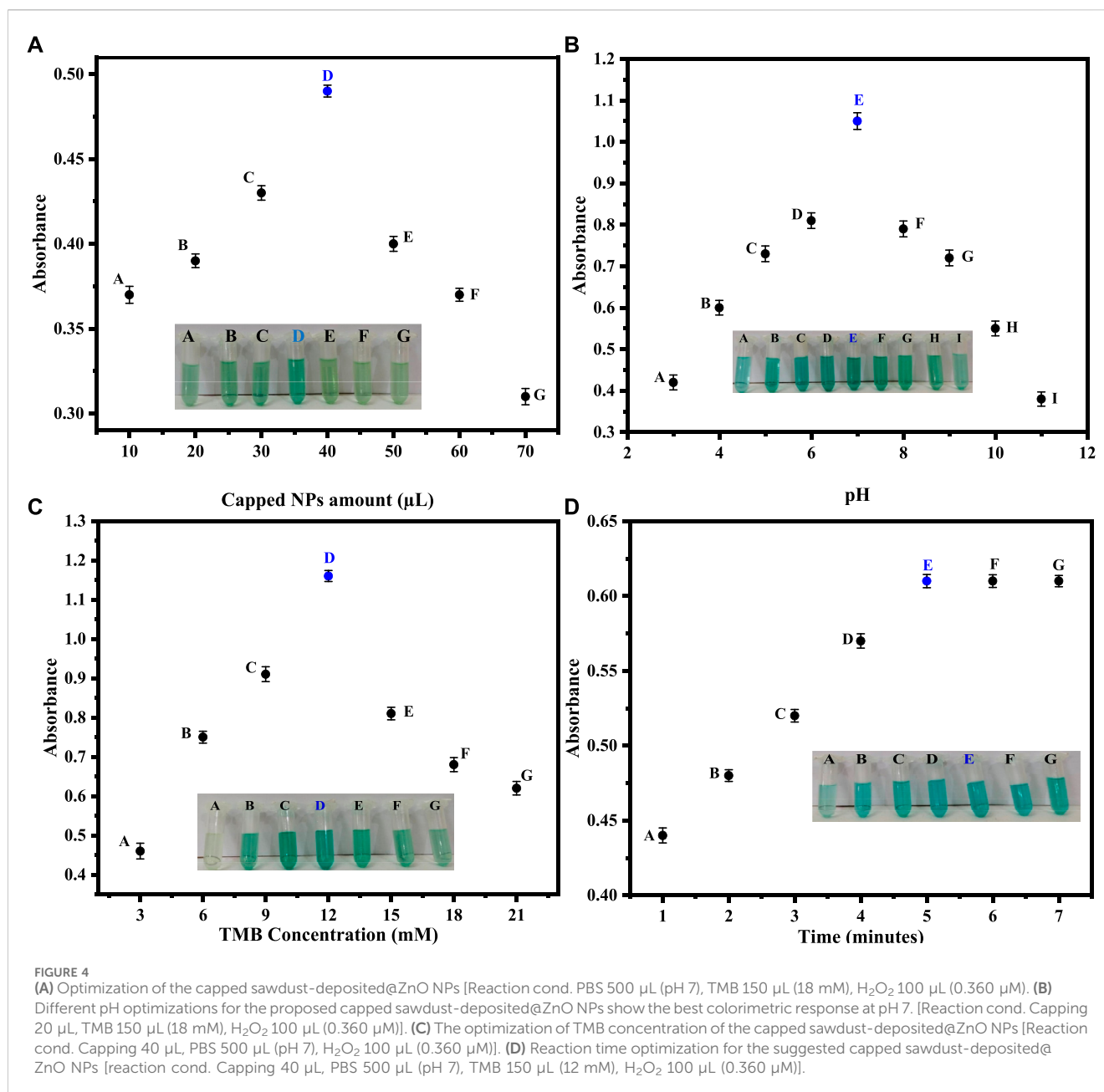
Capped sawdust-deposited@ZnO NPs (25 μL) were suspended in 500 μL phosphate buffer (pH 7), followed by the addition of 150 μL TMB solution (18 mM). Add 90 μL of H<sub>2</sub>O<sub>2</sub> (0.360 μM) to the reaction mixture and incubate at room temperature for the colorimetric reaction. The absorption spectrum of the resultant solution was recorded using a UV-Vis spectrophotometer. Some experimental parameters, such as response time, pH, the amount of capped NPs, and the concentration of TMB solution, have been tuned up to achieve the best results of the proposed platform.

## 3 Results and discussion

### 3.1 Characterization of the sawdust-deposited@ZnO NPs

#### 3.1.1 UV-vis spectroscopy

To investigate the optical characteristics of the sawdust-deposited@ZnO NPs, a UV-Visible spectrophotometer was used. The UV-Vis absorption spectrum of the synthesized sawdust-deposited@ZnO NPs with a peculiar absorption band at 320 nm



is shown in Figure 1A. The fact that ZnO has a considerable, sharp absorption implies that the nanoparticles distribution is monodispersed (Talam et al., 2012).

### 3.1.2 FTIR analysis of the sawdust-deposited@ZnO NPs

FTIR analysis in the range of 4,000–500 cm<sup>-1</sup>, was used to determine the different functional groups found on the surface of the sawdust-deposited@ZnO NPs. The broad absorption band at 3,310 cm<sup>-1</sup> indicates the presence of an OH group from the plant source on the surface of the synthesized platform. The peak around 2,950 cm<sup>-1</sup> shows the C-H stretching vibration of the alkyl group present in the mimic enzyme. The most important characteristic peak around 580 cm<sup>-1</sup> represents the presence of Zn–O bond present

in our synthesized platform, indicating that the ZnO nanoparticles present in the sawdust-deposited@ZnO NPs are as shown in Figure 1B. A similar pattern of peaks has already been reported for ZnO in the literature (Xiong et al., 2006).

### 3.1.3 XRD analysis

The X-ray diffraction pattern of the synthesized sawdust-deposited@ZnO NPs is shown in Figure 1C. The XRD results of the prepared platform centered at 2θ = 21 reveal a diffraction peak with miller indices of 120. When compared to standard data, it was found that the peak matched the hexagonal phase of ZnO NPs standard data (JCPDS card no. 36–1451) (Srivastava et al., 2013). The average crystal size of orthorhombic-phase ZnO NPs was calculated to be about 35 nm using Scherrer equation.

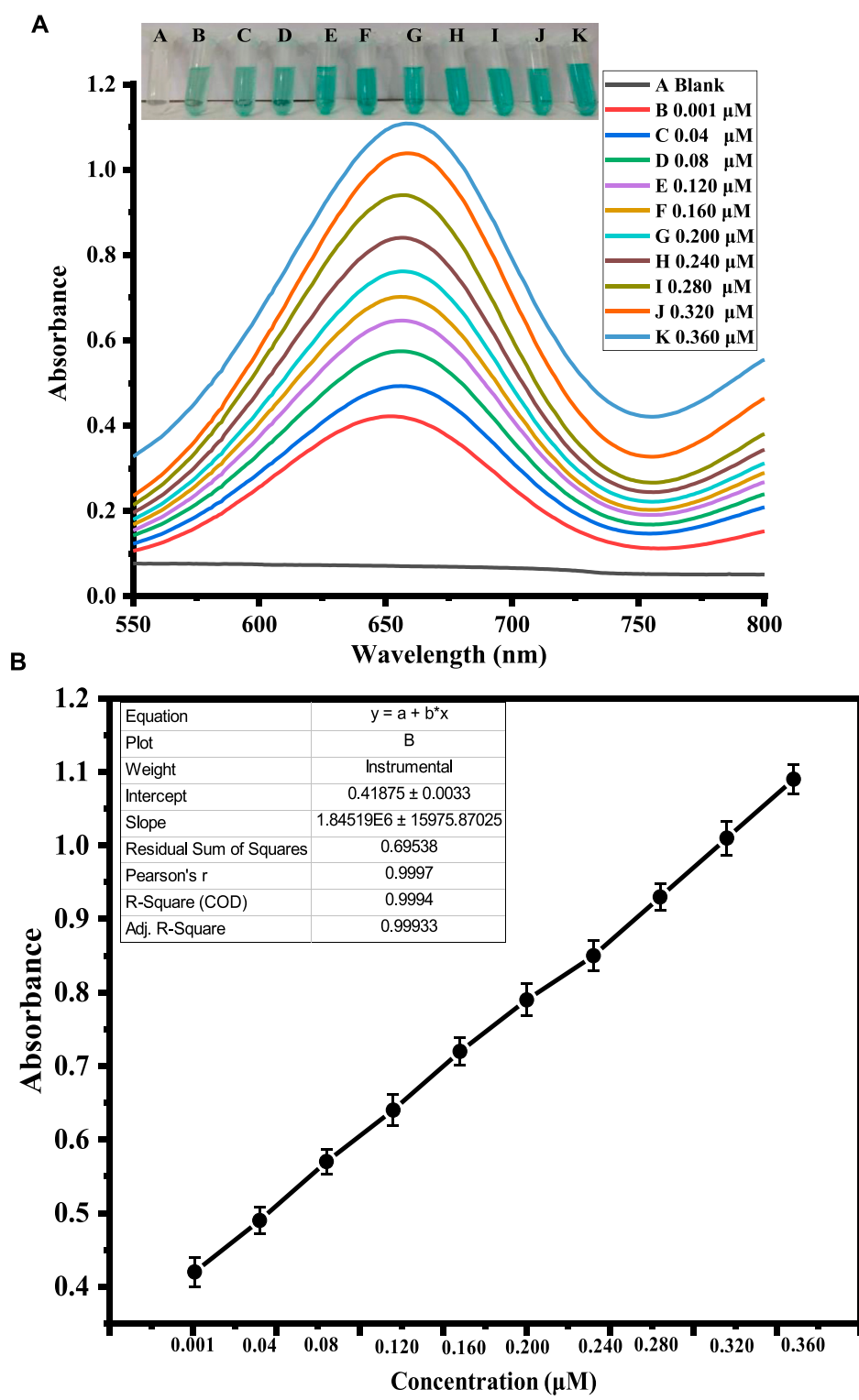


**FIGURE 5** Shows the optimization of H<sub>2</sub>O<sub>2</sub> concentration. Figure (A) shows the UV-Vis response recorded at different concentrations of H<sub>2</sub>O<sub>2</sub>. The inset figure shows varying color changes with the addition of different concentrations of H<sub>2</sub>O<sub>2</sub>. Figure (B) shows the corresponding calibration curve of the absorbance at different H<sub>2</sub>O<sub>2</sub> concentrations.

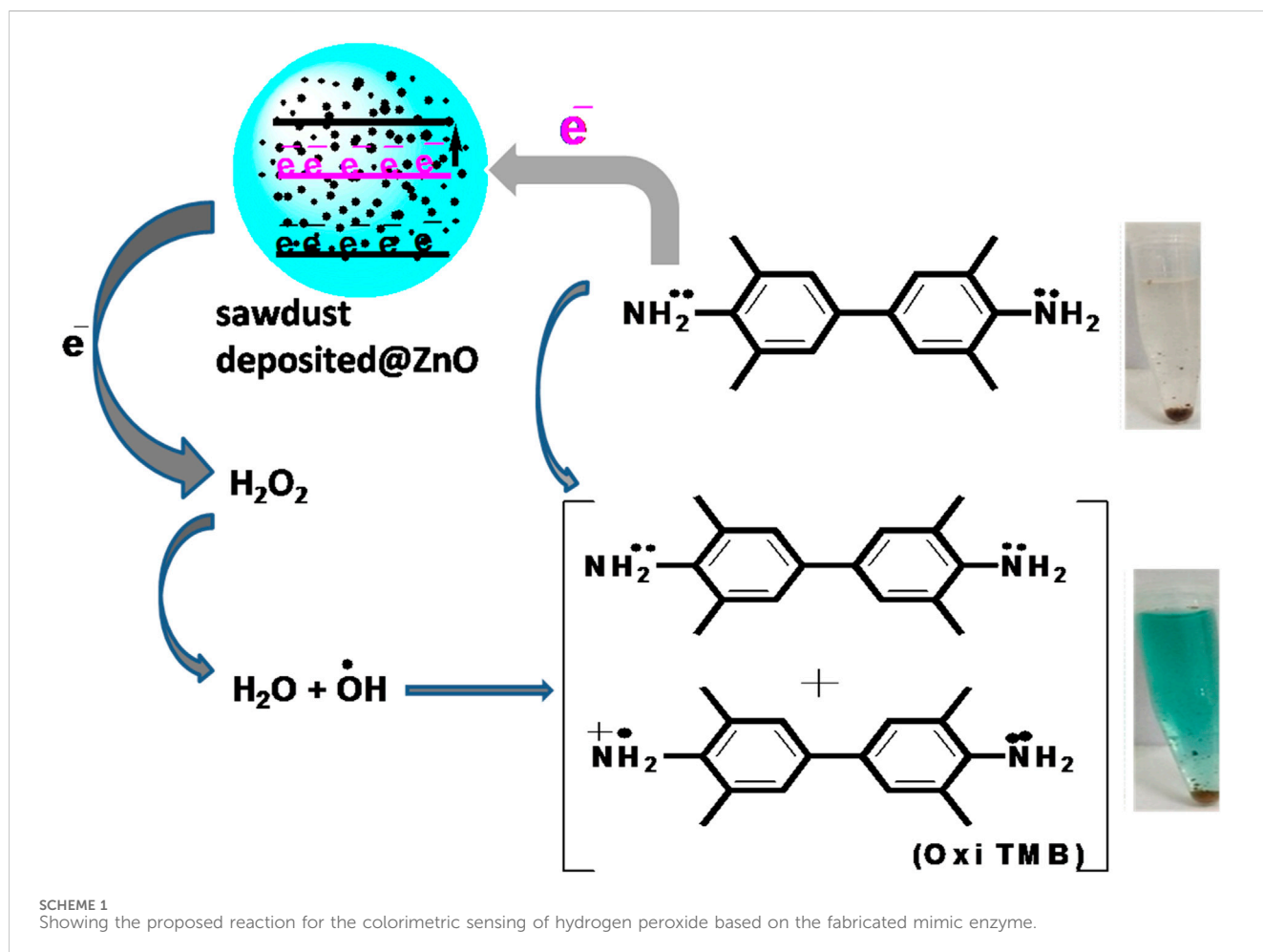
### 3.1.4 EDX analysis

The chemical composition of the sawdust-deposited@ZnO NPs was examined using EDX analysis, as shown in Figure 1D and

Table 1. The results showed the presence of Zn and O in the sawdust-deposited@ZnO sample. In addition to Zn and O, some other elements like Ca and C are also present. The percent contents

TABLE 2 Comparison of different colorimetric biosensors for H<sub>2</sub>O<sub>2</sub>.

S. No.	Materials used	Method applied	Linear range (μM)	Limit of detection (μM)	References
1	CuS	Colorimetric	1–1,000	0.11	Guan et al. (2015)
2	PB NPs	Colorimetric	0.1–50	0.031	Zhang et al. (2014)
3	Ag NPs	Colorimetric	0.01–30	0.014	Teodoro et al. (2019)
4	RhNPs	Colorimetric	1–100	0.75	Choleva et al. (2018)
5	Cu(II)-coated Fe <sub>3</sub> O <sub>4</sub> NPs	Colorimetric	2.5–100	0.2	Liu et al. (2019)
6	GQDs/CuO	Colorimetric	0.5–10	0.17	Zhang et al. (2017)
7	ZV-Mn NPs	Colorimetric	10–280	0.2	Rauf et al. (2020)
8	FeCDs	Colorimetric	6–42	0.93	Bandi et al. (2021)
9	Ni NPs	Colorimetric	400–4,000	120	Zarif et al. (2020)
10	TiO <sub>2</sub> NPs	Colorimetric	0.001–0.360	0.08	Nishan et al. (2021a)
11	lignin-based Ag NPs	Colorimetric	0.001–0.360	0.0137	Nishan et al. (2021b)
12	Ag-Fe <sub>2</sub> O <sub>3</sub> NPs	Colorimetric	0.001–0.320	0.0107	Nishan et al. (2023)
13	Capped sawdust-deposited@ZnO NPs	Colorimetric	0.001–0.360	0.00024	This work



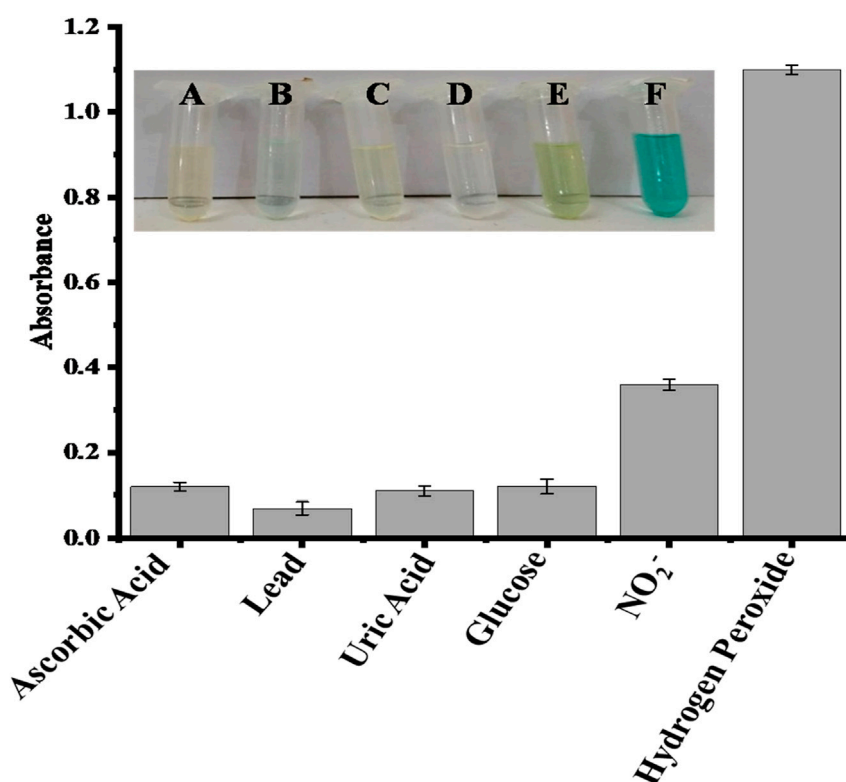


FIGURE 6

Comparative interference study of the proposed capped sawdust-deposited@ZnO NPs sensor for the detection of hydrogen peroxide with other analytes, indicating high selectivity of the proposed platform for the sensing of H<sub>2</sub>O<sub>2</sub>. In the inset Figure, the letters A, B, C, D, E, and F represent ascorbic acid, lead, uric acid, glucose, nitrite, and hydrogen peroxide, respectively.

of Zn, O, C, and Ca are 3.64, 46.95, 49.90, and 0.17, respectively, by weight as shown in the table.

### 3.1.5 SEM analysis

To investigate the surface morphology of the synthesized sawdust-deposited@ZnO NPs, SEM images of different resolutions were taken, as shown in Figure 2A–D. SEM images confirmed that the prepared ZnO NPs are distributed uniformly over the surface of sawdust. This uniform distribution of the nanoparticles is highly desirable and helpful in terms of the surface area of the nanoparticles for their catalytic activity.

## 3.2 Colorimetric detection of H<sub>2</sub>O<sub>2</sub>

H<sub>2</sub>O<sub>2</sub> sensing by the proposed sawdust-deposited@ZnO NPs was done using a very simple and highly selective colorimetric approach. The optical sensing and UV-Vis absorption spectra are shown in Figure 3. When H<sub>2</sub>O<sub>2</sub> is introduced to the sensor system, it produces a blue-green color from the colorless TMB. Mechanistically, adsorption of H<sub>2</sub>O<sub>2</sub> on the surface of NPs produces OH radicals, which oxidize the colorless TMB substrate into a blue-green product, as can be seen with the naked eye, as shown in Figure. The colorimetric change was confirmed by a UV-Vis spectrophotometer. To confirm that the colorimetric change was due to the synthesized sawdust-deposited@ZnO NPs, we used *M. nigra* sawdust without ZnO NPs as a negative control. When H<sub>2</sub>O<sub>2</sub> was added, no color change was detected; indicating that the color change was caused only by

the capped sawdust-deposited@ZnO NPs. UV-Vis spectroscopic investigation validated the negative control experiment, as indicated in Figure.

## 3.3 Proposed mechanism of the reaction

In the current work, mimic enzyme (acetic acid-capped ZnO NPs deposited sawdust) receive electrons from TMB. It results in an increase in the conductivity of electrons in the mimic enzyme, which provides an active site for the proposed chemical reaction. The mobility of electrons results in the transfer of electrons to H<sub>2</sub>O<sub>2</sub>. It results in the generation of hydroxyl free radicals. The generated hydroxyl free radicals oxidize the TMB, resulting in the formation of a blue-green complex. This colorimetric change is visible to the naked eye and was also confirmed with a UV-Vis spectrophotometer. The maximum absorption was found to be at 652 nm. The detailed proposed reaction can be seen in Scheme 1.

## 3.4 Optimization of parameters

### 3.4.1 Amount of capped ZnO NPs

In order to get the best colorimetric response, we first optimized the amount of capped sawdust-deposited@ZnO NPs. Briefly, different amounts (10–70 μL) of the capped sawdust-deposited@



TABLE 3 Detection of hydrogen peroxide in blood serum sample of diabetes patient (n = 3).

Samples	Detected ( $\mu\text{M}$ )	$\text{H}_2\text{O}_2$ added ( $\mu\text{M}$ )	$\text{H}_2\text{O}_2$ found ( $\mu\text{M}$ )	Recovery (%)	RSD (%)
1	0.004	0.017	0.021	123.53	0.271
2	0.007	0.120	0.127	105.83	0.451
3	0.013	0.206	0.219	106.31	0.214

ZnO NPs were tested, and the best colorimetric response was obtained at a 40  $\mu\text{L}$  concentration, as shown in Figure 4A. No significant colorimetric response was obtained below 40  $\mu\text{L}$ , so the 40  $\mu\text{L}$  amount was taken as the optimum amount for further experiments. Previously, we reported about 25  $\mu\text{L}$  of capped  $\text{TiO}_2$  NPs as an optimum concentration for the colorimetric sensing of  $\text{H}_2\text{O}_2$  (Nishan et al., 2021a). Under the given conditions, an increase in the concentration of the mimic enzyme from 40  $\mu\text{L}$  up to 70  $\mu\text{L}$  results in a lower response. This can possibly be explained by the fact that unreacted mimic enzyme interferes with the already oxidized TMB, resulting in much lower absorption.

### 3.4.2 pH optimization

Different pH optimizations were done to get the maximum colorimetric response. Briefly, different pH solutions of PBS were made, and their respective pH values were adjusted using sodium hydroxide and hydrochloric acid solutions. The best colorimetric response shown by the capped sawdust-deposited@ZnO NPs was recorded on pH 7, as shown in Figure 4B. No significant colorimetric response was noticed above or below this optimum pH of 7, therefore pH 7 was selected as the optimum pH for further experiments. At a lower pH, the concentration of hydrogen ions increases, which results in the protonation of the amino group of the chromogenic substrate TMB. This protonation of TMB makes it less susceptible to oxidation, resulting in a lower colorimetric change. The increase in pH above 7 results in an increase in hydroxyl ion

concentration. As a result, the oxidation of TMB reduces, and hence less colorimetric change can be observed. Similarly an earlier study reported pH 7.5 to be optimum for the colorimetric sensing of hydrogen peroxide (Nishan et al., 2021b).

### 3.4.3 Optimization of TMB concentration

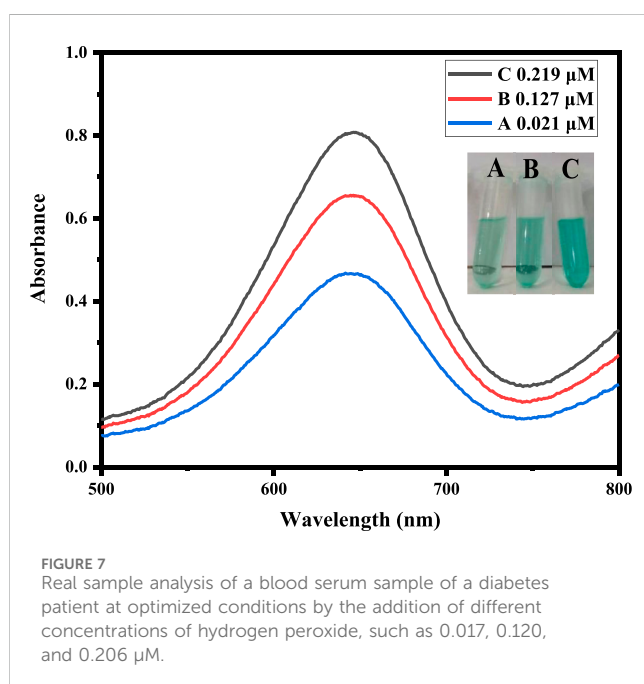
TMB solutions of different concentrations ranging from 3 to 21 mM were prepared. Initially, the colorimetric response increased up to 12 mM and then decreased as the concentration of TMB increased from 13 mM to 21 mM. The best colorimetric response was noticed at 12 mM, as shown in Figure 4C. Recently, for the detection of hydrogen peroxide, the 8 mM optimum TMB concentration was reported by our groups for another nanostructure (Nishan et al., 2023). This could possibly be explained by the fact that in the reported work, a pristine form of nanomaterial functionalized with ionic liquid was used as a mimic enzyme. In the current work, sawdust was used as a matrix material, hence the higher concentration of TMB.

### 3.4.4 Optimization of time

In colorimetric detection of hydrogen peroxide, the reaction incubation time was also optimized. A colorimetric response was noticed at various time intervals (1–7 min) after adding hydrogen peroxide. The reaction time at various intervals was recorded by UV-Vis spectroscopy. After 5 min, no further change in color or absorbance was noticed, indicating that 5 min is the optimal time for a complete reaction, as shown in Figure 4D. According to the literature, the optimum time for the detection of hydrogen peroxide was 10 min, as reported by (Zarif et al., 2020), which is much higher than our present work.

## 3.5 Optimization of hydrogen peroxide concentration

$\text{H}_2\text{O}_2$  was detected using a quick and easy colorimetric method based on capped sawdust-deposited@ZnO NPs under ideal experimental circumstances. As seen in Figure 5, the developed biosensor's sensitivity for  $\text{H}_2\text{O}_2$  detection was tested using a range of  $\text{H}_2\text{O}_2$  concentrations. At lower  $\text{H}_2\text{O}_2$  concentrations, the sensor response and peak intensity were negligible, but as the concentration rose, they grew linearly.  $\text{H}_2\text{O}_2$  detection with an  $R^2$  value of 0.999 and a linear range of 0.001–0.360  $\mu\text{M}$  was made possible by this method. It was determined that the limits of quantification (LOQ) and detection (LOD) were, respectively, 0.24 nM and 0.81 nM. The suggested colorimetric approach had the advantages of a low detection limit, low cost, and naked eye observation over other previously published detection methods. Based on the linear range and limit of detection, we compared



this work for H<sub>2</sub>O<sub>2</sub> detection with previously reported colorimetric approaches, as shown in Table 2. It is clear from the results that the fabricated sensor showed an exceptional limit of detection and a comparable wide linear range with previous works from our group.

### 3.6 Selectivity analysis the proposed sensor

The potential interfering chemicals, including ascorbic acid, lead, uric acid, glucose, and nitrite, were used to test the selectivity of the proposed sensor. All these interfering chemicals had substantially lower absorbance than H<sub>2</sub>O<sub>2</sub>, as shown in Figure 6. The recorded absorbance was highest when H<sub>2</sub>O<sub>2</sub> was added, and no significant absorbance change was seen when a co-existing material was added. In the presence of higher amounts of ascorbic acid, lead, uric acid, glucose, and nitrite ions, the suggested sensor has a substantially stronger selectivity for H<sub>2</sub>O<sub>2</sub>. All the experiments were performed in the presence of 0.360 μM H<sub>2</sub>O<sub>2</sub> and a double concentration of other interfering substances.

### 3.7 Real sample analysis

To assess the practical application of the proposed sensor to detect H<sub>2</sub>O<sub>2</sub> content, the measurement of H<sub>2</sub>O<sub>2</sub> in the blood serum sample of a diabetes patient was carried out as shown in Table 3. The present amount of H<sub>2</sub>O<sub>2</sub> was calculated from the already calibrated graph by using the spiking method. Different concentrations of H<sub>2</sub>O<sub>2</sub> solution, such as 0.017, 0.120, and 0.206 μM, were spiked into the blood serum sample of a diabetes patient and analyzed, as shown in Figure 7. The results demonstrated that the H<sub>2</sub>O<sub>2</sub> concentrations in the real samples determined by the current assay are in good agreement with the spiked H<sub>2</sub>O<sub>2</sub> concentrations.

## 4 Conclusion

*Morus nigra*-deposited ZnO@NPs were successfully synthesized from *T. foenum* extract. The synthesized platform was characterized with various standard analytical techniques, including FTIR, SEM, XRD, and EDX. The synthesized sawdust-deposited@ZnO NPs were capped with acetic acid and successfully used for the colorimetric sensing of H<sub>2</sub>O<sub>2</sub>. Our current finding demonstrates that acetic acid-capped sawdust-deposited@ZnO NPs show enhanced intrinsic peroxidase-like activity. The proposed platform showed good sensitivity and selectivity in the presence of a double amount of potential interfering species. The fabricated platform shows a number of advantages over natural enzymes, including easy preparation, low cost, quick reaction times, and high stability. These advantages make it a suitable candidate peroxidase-mimic for future applications in biotechnology, medical diagnostics, and hydrogen peroxide monitoring.

### Data availability statement

The raw data supporting the conclusion of this article will be made available by the authors, without undue reservation.

## Author contributions

UN: Conceptualization, Formal Analysis, Investigation, Project administration, Supervision, Writing–original draft, Writing–review and editing. TZ: Data curation, Investigation, Methodology, Writing–original draft. AB: Investigation, Methodology, Project administration, Supervision, Visualization, Writing–review and editing. NM: Conceptualization, Formal Analysis, Methodology, Visualization, Writing–review and editing. SA: Data curation, Formal Analysis, Investigation, Validation, Writing–review and editing. MS: Data curation, Investigation, Software, Writing–original draft. NK: Formal Analysis, Methodology, Validation, Visualization, Writing–review and editing. MA: Data curation, Formal Analysis, Investigation, Methodology, Software, Writing–original draft. RU: Funding acquisition, Investigation, Project administration, Resources, Software, Visualization, Writing–review and editing. EA: Formal Analysis, Funding acquisition, Methodology, Project administration, Resources, Visualization, Writing–original draft. KC: Conceptualization, Funding acquisition, Investigation, Methodology, Project administration, Resources, Supervision, Writing–original draft, Writing–review and editing.

## Funding

The author(s) declare financial support was received for the research, authorship, and/or publication of this article. This research work is supported by the Doctoral research fund of the Affiliated Hospital of Southwest Medical University, Luzhou 646000, China, awarded to KC. The authors thank researchers supporting Project number (RSP2024R110) King Saud University, Riyadh, Saudi Arabia.

## Acknowledgments

KC acknowledges the doctoral research fund of the Affiliated Hospital of Southwest Medical University, Luzhou 646000, China. Authors wish to thanks Researchers Supporting Project Number (RSP2024R110) at King Saud University Riyadh Saudi Arabia for financial support.

## Conflict of interest

The authors declare that the research was conducted in the absence of any commercial or financial relationships that could be construed as a potential conflict of interest.

## Publisher's note

All claims expressed in this article are solely those of the authors and do not necessarily represent those of their affiliated organizations, or those of the publisher, the editors and the reviewers. Any product that may be evaluated in this article, or claim that may be made by its manufacturer, is not guaranteed or endorsed by the publisher.

## References

- Abou Chaaya, A., Bechelany, M., Balme, S., and Miele, P. (2014). ZnO 1D nanostructures designed by combining atomic layer deposition and electrospinning for UV sensor applications. *J. Mater. Chem. A* 2, 20650–20658. doi:10.1039/c4ta05239k
- Asad, M., Muhammad, N., Khan, N., Shah, M., Khan, M., Khan, M., et al. (2022). Colorimetric acetone sensor based on ionic liquid functionalized drug-mediated silver nanostructures. *J. Pharm. Biomed. Analysis* 221, 115043. doi:10.1016/j.jpba.2022.115043
- Bandi, R., Alle, M., Park, C.-W., Han, S.-Y., Kwon, G.-J., Kim, N.-H., et al. (2021). Cellulose nanofibrils/carbon dots composite nanopapers for the smartphone-based colorimetric detection of hydrogen peroxide and glucose. *Sensors Actuators B Chem.* 330, 129330. doi:10.1016/j.snb.2020.129330
- Chen, W., Chen, J., Liu, A. L., Wang, L. M., Li, G. W., and Lin, X. H. (2011). Peroxidase-like activity of cupric oxide nanoparticle. *ChemCatChem* 3, 1151–1154. doi:10.1002/cctc.201100064
- Chen, X., Wu, G., Cai, Z., Oyama, M., and Chen, X. (2014). Advances in enzyme-free electrochemical sensors for hydrogen peroxide, glucose, and uric acid. *Microchim. Acta* 181, 689–705. doi:10.1007/s00604-013-1098-0
- Choleva, T. G., Gatselou, V. A., Tsogas, G. Z., and Giokas, D. L. (2018). Intrinsic peroxidase-like activity of rhodium nanoparticles, and their application to the colorimetric determination of hydrogen peroxide and glucose. *Microchim. Acta* 185, 22–29. doi:10.1007/s00604-017-2582-8
- Dutta, A. K., Das, S., Samanta, S., Samanta, P. K., Adhikary, B., and Biswas, P. (2013). CuS nanoparticles as a mimic peroxidase for colorimetric estimation of human blood glucose level. *Talanta* 107, 361–367. doi:10.1016/j.talanta.2013.01.032
- Guan, J., Peng, J., and Jin, X. (2015). Synthesis of copper sulfide nanorods as peroxidase mimics for the colorimetric detection of hydrogen peroxide. *Anal. Methods* 7, 5454–5461. doi:10.1039/c5ay00895f
- Irani-nezhad, M. H., Khataee, A., Hassanzadeh, J., and Orooji, Y. (2019). A chemiluminescent method for the detection of H<sub>2</sub>O<sub>2</sub> and glucose based on intrinsic peroxidase-like activity of WS<sub>2</sub> quantum dots. *Molecules* 24, 689. doi:10.3390/molecules24040689
- Jv, Y., Li, B., and Cao, R. (2010). Positively-charged gold nanoparticles as peroxidase mimic and their application in hydrogen peroxide and glucose detection. *Chem. Commun.* 46, 8017–8019. doi:10.1039/c0cc02698k
- Khalqi, A., Nazir, R., Khan, M., Rahim, A., Asad, M., Shah, M., et al. (2023). Co-doped CeO<sub>2</sub>/activated C nanocomposite functionalized with ionic liquid for colorimetric biosensing of H<sub>2</sub>O<sub>2</sub> via peroxidase mimicking. *Molecules* 28, 3325. doi:10.3390/molecules28083325
- Khranovskyy, V., Lazorenko, V., Lashkarev, G., and Yakimova, R. (2012). Luminescence anisotropy of ZnO microrods. *J. Luminescence* 132, 2643–2647. doi:10.1016/j.jlumin.2012.04.048
- Lee, J. H., Huynh-Nguyen, B.-C., Ko, E., Kim, J. H., and Seong, G. H. (2016). Fabrication of flexible, transparent silver nanowire electrodes for amperometric detection of hydrogen peroxide. *Sensors Actuators B Chem.* 224, 789–797. doi:10.1016/j.snb.2015.11.006
- Liu, H., Zhu, L., Ma, H., Wen, J., Xu, H., Qiu, Y., et al. (2019). Copper (II)-coated Fe<sub>3</sub>O<sub>4</sub> nanoparticles as an efficient enzyme mimic for colorimetric detection of hydrogen peroxide. *Microchim. Acta* 186, 518–519. doi:10.1007/s00604-019-3599-y
- Miller, E. W., Dickinson, B. C., and Chang, C. J. (2010). Aquaporin-3 mediates hydrogen peroxide uptake to regulate downstream intracellular signaling. *Proc. Natl. Acad. Sci.* 107, 15681–15686. doi:10.1073/pnas.1005776107
- Nakashima, K., Wada, M., Kuroda, N., Akiyama, S., and Imai, K. (1994). High-performance liquid chromatographic determination of hydrogen peroxide with peroxyoxalate chemiluminescence detection. *J. Liq. Chromatogr. Relat. Technol.* 17, 2111–2126. doi:10.1080/10826079408013535
- Nishan, U., Haq, S. U., Rahim, A., Asad, M., Badshah, A., Ali Shah, A.-u.-H., et al. (2021a). Ionic-liquid-stabilized TiO<sub>2</sub> nanostructures: a platform for detection of hydrogen peroxide. *ACS omega* 6, 32754–32762. doi:10.1021/acsomega.1c04548
- Nishan, U., Khan, H. U., Rahim, A., Asad, M., Qayum, M., Khan, N., et al. (2022). Non-enzymatic colorimetric sensing of nitrite in fortified meat using functionalized drug mediated manganese dioxide. *Mater. Chem. Phys.* 278, 125729. doi:10.1016/j.matchemphys.2022.125729
- Nishan, U., Niaz, A., Muhammad, N., Asad, M., Khan, N., Khan, M., et al. (2021b). Non-enzymatic colorimetric biosensor for hydrogen peroxide using lignin-based silver nanoparticles tuned with ionic liquid as a peroxidase mimic. *Arabian J. Chem.* 14, 103164. doi:10.1016/j.arabj.2021.103164
- Nishan, U., Ullah, I., Muhammad, N., Afridi, S., Asad, M., Haq, S. U., et al. (2023). Investigation of silver-doped iron oxide nanostructures functionalized with ionic liquid for colorimetric sensing of hydrogen peroxide. *Arabian J. Sci. Eng.* 48, 7703–7712. doi:10.1007/s13369-023-07791-z
- Ornatska, M., Sharpe, E., Andreescu, D., and Andreescu, S. (2011). Paper bioassay based on ceria nanoparticles as colorimetric probes. *Anal. Chem.* 83, 4273–4280. doi:10.1021/ac200697y
- Park, N.-M., Choi, S., Oh, J. E., and Hwang, D. Y. (2019). Facile extraction of cellulose nanocrystals. *Carbohydr. Polym.* 223, 115114. doi:10.1016/j.carbpol.2019.115114
- Patel, V., Kruse, P., and Selvaganapathy, P. R. (2020). Solid state sensors for hydrogen peroxide detection. *Biosensors* 11 (9), 9. doi:10.3390/bios11010009
- Rao, A., and Balachandran, B. (2002). Role of oxidative stress and antioxidants in neurodegenerative diseases. *Nutr. Neurosci.* 5, 291–309. doi:10.1080/1028415021000033767
- Rauf, S., Ali, N., Tayyab, Z., Shah, M. Y., Yang, C. P., Hu, J., et al. (2020). Ionic liquid coated zerovalent manganese nanoparticles with stabilized and enhanced peroxidase-like catalytic activity for colorimetric detection of hydrogen peroxide. *Mater. Res. Express* 7, 035018. doi:10.1088/2053-1591/ab7f10
- Senthamizhan, A., Balusamy, B., Aytac, Z., and Uyar, T. (2016). Ultrasensitive electrospun fluorescent nanofibrous membrane for rapid visual colorimetric detection of H<sub>2</sub>O<sub>2</sub>. *Anal. Bioanal. Chem.* 408, 1347–1355. doi:10.1007/s00216-015-9149-5
- Shi, W., Zhang, X., He, S., and Huang, Y. (2011). CoFe<sub>2</sub>O<sub>4</sub> magnetic nanoparticles as a peroxidase mimic mediated chemiluminescence for hydrogen peroxide and glucose. *Chem. Commun.* 47, 10785–10787. doi:10.1039/c1cc14300j
- Singh, J., Singh, R., Singh, S., Mitra, K., Mondal, S., Vishwakarma, S., et al. (2022). Colorimetric detection of hydrogen peroxide and cholesterol using Fe<sub>3</sub>O<sub>4</sub>-brominated graphene nanocomposite. *Anal. Bioanal. Chem.* 414, 2131–2145. doi:10.1007/s00216-021-03848-w
- Song, Y., Qu, K., Zhao, C., Ren, J., and Qu, X. (2010). Graphene oxide: intrinsic peroxidase catalytic activity and its application to glucose detection. *Adv. Mater.* 22, 2206–2210. doi:10.1002/adma.200903783
- Srivastava, V., Gusain, D., and Sharma, Y. C. (2013). Synthesis, characterization and application of zinc oxide nanoparticles (n-ZnO). *Ceram. Int.* 39, 9803–9808. doi:10.1016/j.ceramint.2013.04.110
- Talam, S., Karumuri, S. R., and Gunnam, N. (2012). Synthesis, characterization, and spectroscopic properties of ZnO nanoparticles. *Int. Sch. Res. Notices* 2012, 1–6. doi:10.5402/2012/372505
- Teodoro, K. B., Migliorini, F. L., Christinelli, W. A., and Correa, D. S. (2019). Detection of hydrogen peroxide (H<sub>2</sub>O<sub>2</sub>) using a colorimetric sensor based on cellulose nanowhiskers and silver nanoparticles. *Carbohydr. Polym.* 212, 235–241. doi:10.1016/j.carbpol.2019.02.053
- Wei, Y., Li, Y., Liu, X., Xian, Y., Shi, G., and Jin, L. (2010). ZnO nanorods/Au hybrid nanocomposites for glucose biosensor. *Biosens. Bioelectron.* 26, 275–278. doi:10.1016/j.bios.2010.06.006
- Xiong, G., Pal, U., Serrano, J., Ucer, K., and Williams, R. (2006). Photoluminescence and FTIR study of ZnO nanoparticles: the impurity and defect perspective. *Phys. status solidi C* 3, 3577–3581. doi:10.1002/pssc.200672164
- Zarif, F., Rauf, S., Khurshid, S., Muhammad, N., Hayat, A., Rahim, A., et al. (2020). Effect of pyridinium based ionic liquid on the sensing property of NiO nanoparticle for the colorimetric detection of hydrogen peroxide. *J. Mol. Struct.* 1219, 128620. doi:10.1016/j.molstruc.2020.128620
- Zhang, L., Hai, X., Xia, C., Chen, X.-W., and Wang, J.-H. (2017). Growth of CuO nanoneedles on graphene quantum dots as peroxidase mimics for sensitive colorimetric detection of hydrogen peroxide and glucose. *Sensors Actuators B Chem.* 248, 374–384. doi:10.1016/j.snb.2017.04.011
- Zhang, W., Ma, D., and Du, J. (2014). Prussian blue nanoparticles as peroxidase mimetics for sensitive colorimetric detection of hydrogen peroxide and glucose. *Talanta* 120, 362–367. doi:10.1016/j.talanta.2013.12.028
- Zhang, W., Niu, X., Li, X., He, Y., Song, H., Peng, Y., et al. (2018). A smartphone-integrated ready-to-use paper-based sensor with mesoporous carbon-dispersed Pd nanoparticles as a highly active peroxidase mimic for H<sub>2</sub>O<sub>2</sub> detection. *Sensors Actuators B Chem.* 265, 412–420. doi:10.1016/j.snb.2018.03.082